VIRULENCE
2025, VOL. 16, NO. 1, 2497903
https://doi.org/10.1080/21505594.2025.2497903

Taylor & Francis
Taylor & Francis Group

HOST RESPONSE

OPEN ACCESS Check for updates

A promising endeavor against human cytomegalovirus: Predominant epitopes-based recombinant subunit vaccine RH*Ec*$^{IE1/pp65/pp150}$

Zonghui Li [a,b*], Shasha Jiang [a,c*], Wenxuan Liu[a], Xiaoli Yang[a], Fengjun Liu[a], Xu Li[a], Jun Li[a], Meng Yu[a], Zhun Wei[d], Bin Wang [a], and Dongmeng Qian [a]

[a]Department of Pathogenic Biology, Department of Special Medicine, School of Basic Medicine, Qingdao University, Qingdao, China; [b]Department of Clinical Laboratory, Chengdu Aerotropolis Asia Heart Hospital, Chengdu, China; [c]Department of Clinical Laboratory, Honghui Hospital, Xi'an Jiaotong University, Xi'an, China; [d]Department of Pharmacology, School of Pharmacy, Qingdao University, Qingdao, China

ABSTRACT

Human cytomegalovirus (HCMV) is widespread in the population, typically remaining latent. However, it can cause severe morbidity and mortality in transplant patients and immunodeficient individuals. Currently, there is no approved vaccine against HCMV. This study used immunoinformatics methods to predict the predominant T and B-cell epitopes of three key HCMV proteins, including phosphoprotein 65 (pp65), pp150, and immediate-early protein 1 (IE1). Subsequently, we synthesized a recombinant subunit vaccine (RH*Ec*$^{IE1/pp65/pp150}$) from *Escherichia coli*, comprising RH*Ec*-1 and RH*Ec*-2. We observed that the RH*Ec*$^{IE1/pp65/pp150}$ vaccine exhibited high safety and immunogenicity in mice, enhancing a significant upregulation of CD80, CD86, CD40, and MHCII on dendritic cells and macrophages. Additionally, the vaccine activated innate immune responses through the NF-κB signalling pathway, triggering $CD4^+$ and $CD8^+$T cells to secrete tumour necrosis factor (TNF)-α, interferon (IFN)-γ, and interleukin (IL)-2, directing the T-cell response towards Th1. Moreover, it stimulated $CD4^+$T cells to secrete IL-4, IL-6, and IL-10, promoting B-cell immunity. Furthermore, the RH*Ec*$^{IE1/pp65/pp150}$ vaccine induced the formation of abundant memory cells and high levels of neutralizing antibody titres, conducive to providing long-lasting protection. Taken together, the RH*Ec*$^{IE1/pp65/pp150}$ vaccine is a promising endeavour against HCMV, and these findings contribute valuable insights to the development of HCMV vaccine candidates.

ARTICLE HISTORY
Received 22 January 2024
Revised 23 December 2024
Accepted 21 April 2025

KEYWORDS
Cytomegalovirus; signaling pathway; recombinant subunit vaccine; predominant epitopes; immunogenicity

Introduction

Human cytomegalovirus (HCMV) is a double-stranded DNA virus belonging to the β-herpesvirus subfamily and is considered an opportunistic pathogen [1]. HCMV is widespread globally, with 60% of infections occurring in developed countries and more than 90% in developing countries [1,2]. It can be transmitted through sexual contact, mother-to-child transmission, whole blood transfusion, or organ transplantation [3,4]. HCMV is one of the major pathogens that cause congenital abnormalities after foetal infection and is often asymptomatic in immunocompetent individuals [5]. However, it establishes lifelong latent infection in monocytes and endothelial cells with latency and reactivation periods [2]. Congenital HCMV infection remains a significant medical and public health concern, as the virus can be transmitted to the foetus through the placenta at any time during pregnancy [6], resulting in serious consequences such as sensorineural hearing loss, cognitive impairment, cerebral palsy, microcephaly, and visual impairment in newborns [7,8].

Currently, drugs used to combat HCMV infection, including ganciclovir, valganciclovir, foscarnet, and cidofovir, target the viral polymerase. Long-term use of these compounds is hampered by dose-related toxicity and cross-resistance [9]. Additionally, letermovir has demonstrated excellent efficacy and safety in phase II and III clinical trials, being able to inhibit HCMV variants resistant to other antiviral drugs. Its toxicity is negligible compared to approved HCMV drugs, making it one of the most promising new candidate drugs [9,10]. A significant challenge in the field of medical virology is the development of preventive vaccines for HCMV infection. An ideal HCMV vaccine should have properties that prevent intrauterine transmission of HCMV and/or the disease. Therefore, the development of HCMV vaccines has been designated a major public health priority [11]. Nevertheless, an approved HCMV vaccine is currently unavailable.

CONTACT Bin Wang wangbin532@126.com; Dongmeng Qian 2257683545@qq.com
*These authors contributed equally to this study.
Supplemental data for this article can be accessed online at https://doi.org/10.1080/21505594.2025.2497903

© 2025 The Author(s). Published by Informa UK Limited, trading as Taylor & Francis Group.
This is an Open Access article distributed under the terms of the Creative Commons Attribution-NonCommercial License (http://creativecommons.org/licenses/by-nc/4.0/), which permits unrestricted non-commercial use, distribution, and reproduction in any medium, provided the original work is properly cited. The terms on which this article has been published allow the posting of the Accepted Manuscript in a repository by the author(s) or with their consent.

The HCMV genome encodes over 200 proteins, contributing significantly to immune evasion, viral replication, and viral DNA release [12]. Notably, phosphoprotein 65 (pp65), functioning as a viral structural component, mobilizes strong T-cell responses, and multiple immunodominant epitopes from these antigens have been characterized. Thus, pp65 is considered a potential target for developing candidate vaccines [13,14]. In contrast, pp150, characterized by its high immunogenicity, plays a crucial role in the assembly and excretion of viral particles [15]. Immediate-early 1 (IE1) is one of the proteins that is synthesized de novo after primary HCMV infection or viral reactivation, and is involved in early and late events following HCMV infection. Specifically, IE1 counteracts apoptosis, inhibits signal transduction processes, and antagonizes host antiviral responses that would otherwise terminate the viral lifecycle early on. Therefore, IE1 May offer new opportunities for antiviral intervention [16]. Given the vital role of specific $CD4^+$ and $CD8^+$T cells in controlling HCMV replication, IE1 and pp65 stimulate robust T cell responses. IE1 and pp65 have been used as antigens to induce T-cell responses aimed at inhibiting HCMV infection [13,17].

Recombinant proteins have gained growing significance, being extensively employed and validated for safety in the development of biopharmaceutical products. A diverse array of recombinant proteins with therapeutic and preventive applications has been successfully produced using microorganisms and high-expression host systems. This innovation has paved the way for the development of recombinant subunit vaccines, which play a crucial role in disease prevention and reducing the disease burden. Notably, promising outcomes have been achieved in the prevention and treatment of herpes zoster [18–20].

HCMV infection triggers both humoral and cellular immune responses. Recognizing that solely relying on humoral reactions may not be sufficient to clear the virus and prevent its reactivation [21,22], it is widely believed that cellular immunity controls the majority of HCMV replication. To effectively address HCMV infection, there is a crucial need to target HCMV-specific cellular immune responses [23].

In this context, we hypothesize that candidate vaccines using optimized dominant T and B cell epitopes of key proteins involved in HCMV infection can effectively stimulate the host to generate strong cellular and humoral immune responses against HCMV infection, reducing the incidence and mortality of HCMV-related diseases in immunosuppressed patients, and improving individual quality of life. Using already sequenced HCMV genomes, computational tools, and searchable databases becomes invaluable for predicting potential B and T-cell epitopes. This approach proves more efficient and precise than traditional methods, facilitating vaccine design, immune protein analysis, and immune modelling [24,25]. Consequently, we applied immunoinformatics methods to predict and screen for superior B and T-cell epitope sequences in pp65, pp150, and IE1 of HCMV. Subsequently, we developed a recombinant subunit vaccine (RH*Ec*$^{IE1/pp65/pp150}$), comprising RH*Ec*-1 and RH*Ec*-2, using *Escherichia coli* (*E. coli*) expression. We found that the RH*Ec*$^{IE1/pp65/pp150}$ vaccine was safe and highly immunogenic in mice, and could effectively activate innate and adaptive immune responses. This research introduces a novel and promising design for the development of candidate HCMV vaccines.

Materials and methods

Screening of predominant epitopes

The amino acid sequences of HCMV IE1, pp65, and pp150 proteins were obtained from GenBank (https://www.ncbi.nlm.nih.gov/genbank/). Predictions of dominant T and B-cell epitopes for IE1, pp65, and pp150 proteins were conducted using the SYFPEITHI (http://www.syfpeithi.de/) and the Immune Epitope Database (IEDB) (https://www.iedb.org) [26]. SYFPEITHI primarily predicts T cell epitopes, while IEDB covers a broader range of immune epitope information, including B-cell and T-cell epitopes. By integrating these two databases, a more accurate and reliable prediction of HCMV antigen epitopes can be achieved [27,28]. In selecting cytotoxic T lymphocyte (CTL) epitopes, the NetMHCpan 4.1 EL in the IEDB database was utilized to predict CTL cell epitopes. The amino acid length was set to 8–14 mers, and 14 human leukocyte antigen (HLA) class I allele sites, namely A2, A24, A1, A3, A11, A68, B44, B7, A23, A26, B35, B38, B8, and B27, covering over 90% of the Chinese population [26,29]. For predicting helper T cell (Th) antigen epitopes, the NetMHCIIpan 4.1 EL in the IEDB database was employed to predict Th cell epitopes. The HLA-DRB1 alleles were chosen, and the amino acid length was set to the default [30]. To enhance the accuracy of epitope screening, the SYFPEITHI database was used to predict T cell epitopes. Both the alleles and the amino acid length were kept at the default settings, and the epitopes were selected from the IEDB database with a rank ≤ 1 and from the SYFPEITHI database with a score ≥ 20, ensuring overlap for candidate epitopes [12,31]. B cell epitopes were predicted using the Bepipred Linear Epitope Prediction 2.0 method within IEBD, selecting epitopes with a score greater than 0.5 [12,31–34].

The GGSGGGSGS linker, characterized by high flexibility, provides both sufficient spatial separation and low immunogenicity, while also enhancing the solubility of the vaccine structure in an aqueous milieu. Target sequences were obtained by linking the dominant epitopes with GGSGGGSGS. Wuhan GeneCreate Biological Engineering Company (China) was commissioned to divide the target sequence into two segments, synthesize plasmids with pET22b vectors, and introduce them into *E. coli* for expression. Recombinant *E. coli* colonies resistant to ampicillin were then screened. Subsequently, the recombinant proteins with His tags were purified using a nickel column. After removing endotoxins, the target proteins were dissolved in a buffer solution containing 10 mm Tris-HCl, 1 mm EDTA, pH 8.0, at a concentration of 0.5 mg/mL with a purity over 90%. They were then stored at − 80°C and labelled as RH*Ec*-1 and RH*Ec*-2. The recombinant subunit vaccine RH$Ec^{IE1/pp65/pp150}$ comprises RH*Ec*-1 and RH*Ec*-2. The screening data for IE1, pp65, and pp150 epitopes are presented in Tables 1–3. The amino acid sequence of RH*Ec*-1 is: MSLQFIGLQRRDVVALVNFLRHLTQKPDVDLEA-HPKILKKCGEKRLHRRTVLFNELMLWLGYYGGSG-GGSGSVRHDAEIVERALVSAVILAKMSVGGSGGG-SGSVYTGRLIMNVRRSWEELERKCLGGSGGGSGS-GGGSAFSSVPKKHVPTQPLDGGSGGGSGSQRHAA-FSLVSPQVTKASPGRVRRDSAWDVRPLTETRGGS-GGGSGSITDTETSAKPPVTTAYKGGSGGGSGSSQ-NTVSTTPRRPSTPRAAVTQTASRDAADEVWALR. The amino acid sequence of RH*Ec*-2 is: SPMTTTSTSQKPVLGKRVATPHASARAQTVTSTPV-QGRLEKGGSGGGSGSSMLSSASPSPAKSAPPSPVKGR-GSRVGVPSLKGGSGGGSGSSRAASTTPTYPAVTTVY-PPSSTAKSSVSNAPPVASPSILKPGGGSGGGSGSGS-AGMGGAKTPSDAVQNILQKIEKGGSGGGSGSEP-MSIYVYALPLKMLNIPSINVHHYGGSGGGSGSISHI-MLDVAFTSHEHGGSGGGSGSYQEFFWDANDIYRI-FGGSGGGSGSQIKVRVDMVRHRIKEHMLKKGGS-GGGSGSMLAKRPLITKPEVISVMKRRIEEICMKVF-AQY.

Table 1. Prediction of IE1 epitopes.

HCMV antigen	Start-end	Epitopes	HLA allele	IEDB score	SYFPEITHI score
CTL cell epitopes	88–96	QIKVRVDMV	B*08:01	0.29	24
	92–101	RVDMVRHRIK	A*03:01	0.47	24
	92–101	RVDMVRHRIK	A*11:01	0.6	20
	99–107	RIKEHMLKK	A*03:01	0.01	27
	99–107	RIKEHMLKK	A*11:01	0.08	20
	323–332	MLAKRPLITK	A*03:01	0.05	25
	323–332	MLAKRPLITK	A*11:01	0.4	21
	330–338	ITKPEVISV	A*02:01	0.11	23
	324–332	LAKRPLITK	A*68:01	0.98	21
	343–351	IEEICMKVF	B*44:02	0.63	23
	342–350	RIEEICMKV	A*02:01	0.86	21
	345–354	EICMKVFAQY	A*26:01	0.07	25
	344–354	EEICMKVFAQY	B*44:02	0.13	27
	334–342	EVISVMKRR	A*68:01	0.01	23
	334–342	EVISVMKRR	A*26:01	0.32	25
Th cell epitopes	332–346	KPEVISVMKRRIEEI	DRB1*11:01	0.56	23
B cell epitopes	327–334	RPLITKPE	/	0.5	/

Table 2. Prediction of pp65 epitopes.

HCMV antigen	Start-end	Epitopes	HLA allele	IEDB score	SYFPEITHI score
CTL cell epitopes	110–119	SIYVYALPLK	A*11:01	0.33	22
	110–119	SIYVYALPLK	A*03:01	0.18	23
	113–121	VYALPLKML	A*24:02	0.06	22
	115–123	ALPLKMLNI	A*02:01	0.65	22
	120–128	MLNIPSINV	A*02:01	0.25	22
	119–128	KMLNIPSINV	A*02:01	0.26	21
	107–116	EPMSIYVYAL	B*07:02	0.76	24
	511–521	QEFFWDANDIY	B*44:02	0.33	22
	123–131	IPSINVHHY	B*35:01	0.01	20
	293–302	DVAFTSHEHF	A*26:01	0.14	26
	288–296	SHIMLDVAF	B*38:01	0.03	20
	287–296	ISHIMLDVAF	B*38:01	0.65	20
	516–524	DANDIYRIF	A*26:01	0.16	20
B cell epitopes	120–128	MLNIPSINV	/	0.5	/
	121–124	LNIP	/	0.5	/
	507–519	NLKYQEFFWDAND	/	0.5	/

Table 3. Prediction of pp150 epitopes.

HCMV antigen	Start-end	Epitopes	HLA allele	IEDB score	SYFPEITHI score
CTL cell epitopes	2–10	SLQFIGLQR	A*03:01	0.42	24
	2–10	SLQFIGLQR	A*11:01	0.47	21
	12–21	DVVALVNFLR	A*68:01	0.15	22
	10–21	RRDVVALVNFLR	B*27:05	0.55	28
	13–21	VVALVNFLR	A*11:01	0.5	21
	12–20	DVVALVNFL	A*26:01	0.17	35
	15–23	ALVNFLRHL	A*02:01	0.15	27
	32–40	EAHPKILKK	A*68:01	0.06	22
	36–44	KILKKCGEK	A*03:01	0.35	25
	45–52	RLHRRTVL	B*08:01	0.1	24
	45–53	RLHRRTVLF	B*08:01	0.12	21
	44–52	KRLHRRTVL	B*27:02	0.46	27
	48–56	RRTVLFNEL	B*27:05	0.04	27
	44–53	KRLHRRTVLF	B*27:05	0.2	25
	48–57	RRTVLFNELM	B*27:05	0.44	23
	47–56	HRRTVLFNEL	B*27:05	0.77	22
	51–60	VLFNELMLWL	A*02:01	0.32	23
	54–62	NELMLWLGY	B*44:02	0.24	23
	54–63	NELMLWLGYY	B*44:02	0.74	23
	55–63	ELMLWLGYY	A*26:01	0.14	25
	128–136	ALVSAVILA	A*02:01	0.43	20
	129–137	LVSAVILAK	A*03:01	0.05	27
	129–137	LVSAVILAK	A*11:01	0.08	26
	129–137	LVSAVILAK	A*68:01	0.29	20
	128–137	ALVSAVILAK	A*03:01	0.08	27
	128–137	ALVSAVILAK	A*11:01	0.13	25
	117–127	DVRHDAEIVER	A*68:01	0.64	25
	118–127	VRHDAEIVER	B*27:05	0.37	25
	205–213	YTGRLIMNV	A*02:01	0.88	21
	215–223	RSWEELERK	A*11:01	0.13	20
	207–215	GRLIMNVRR	B*27:05	0.07	29
	214–222	RRSWEELER	B*27:05	0.16	27
	217–225	WEELERKCL	B*44:02	0.9	24
	311–320	GSAFSSVPKK	A*11:01	0.06	25
	494–503	SLVSPQVTKA	A*02:01	0.78	22
	494–502	SLVSPQVTK	A*03:01	0.01	29
	494–502	SLVSPQVTK	A*11:01	0.01	24
	493–502	FSLVSPQVTK	A*03:01	0.3	20
	493–502	FSLVSPQVTK	A*11:01	0.22	26
	493–502	FSLVSPQVTK	A*26:01	0.67	21
	555–563	ITDTETSAK	A*11:01	0.3	21
	515–523	DVRPLTETR	A*68:01	0.04	21
	500–510	VTKASPGRVRR	B*07:02	0.07	22
	509–517	RRDSAWDVR	B*35:01	0.55	20
	564–572	PPVTTAYKF	B*44:02	0.73	21
	684–692	AAVTQTASR	A*68:01	0.07	21
	693–702	DAADEVWALR	A*68:01	0.49	23
	674–683	TTPRRPSTPR	A*68:01	0.19	22
	673–683	STTPRRPSTPR	B*07:02	0.01	25
	678–686	RPSTPRAAV	B*07:02	0.19	21
	681–689	TPRAAVTQT	B*07:02	0.14	21
	678–687	RPSTPRAAVT	B*07:02	0.13	20
	675–684	TPRRPSTPRA	B*07:02	0.23	20
	681–690	TPRAAVTQTA	A*03:01	0.07	31
	781–790	RVATPHASAR	A*11:01	0.17	25
	772–780	TSQKPVLGK	A*11:01	0.12	21
	767–775	MTTTSTSQK	A*11:01	0.21	21
	794–802	VTSTPVQGR	A*11:01	0.15	29
	796–805	STPVQGRLEK	A*11:01	0.01	28
	771–780	STSQKPVLGK	A*11:01	0.78	24
	781–790	RVATPHASAR	A*11:01	0.6	20
	793–802	TVTSTPVQGR	A*68:01	0.02	22
	794–802	VTSTPVQGR	B*07:02	0.03	23
	774–784	KPVLGKRVAT	B*35:01	0.84	22
	883–891	KSAPPSPVK	A*11:01	0.01	25
	875–883	SSASPSPAK	A*11:01	0.63	20
	894–903	GSRVGVPSLK	A*11:01	0.27	21
	874–883	LSSASPSPAK	A*26:01	0.3	32
	895–903	SRVGVPSLK	B*35:01	0.85	21
	963–971	PVASPSILK	A*11:01	0.16	28
	963–971	PVASPSILK	A*68:01	0.68	21
	963–971	PVASPSILK	A*03:01	0.01	29
	946–955	TVYPPSSTAK	A*11:01	0.01	21
	946–955	TVYPPSSTAK	A*68:01	0.05	21
	945–955	TTVYPPSSTAK	A*11:01	0.28	23
	938–946	TPTYPAVTT	B*07:02	0.62	21

(*Continued*)

Table 3. (Continued).

HCMV antigen	Start-end	Epitopes	HLA allele	IEDB score	SYFPEITHI score
	962–970	PPVASPSIL	B*27:05	0.89	21
	961–970	APPVASPSIL	B*07:02	0.34	22
	1032–1040	AVQNILQKI	A*03:01	0.77	22
	1036–1044	ILQKIEKIK	A*11:01	0.58	25
	1019–1027	GSAGMGGAK	A*11:01	0.43	20
	1030–1039	SDAVQNILQK	A*68:01	0.17	23
	1031–1039	DAVQNILQK	B*07:02	0.12	22
	1028–1037	TPSDAVQNIL	B*35:01	0.57	21
	1035–1043	NILQKIEKI	B*08:01	0.27	21
Th cell epitopes	311–325	GSAFSSVPKKHVPTQ	DRB1*11:01	0.58	24
B cell epitopes	7–14	GLQRRDVV	/	0.5	/
	24–33	TQKPDVDLEA	/	0.5	/
	42–47	GEKRLH	/	0.5	/

Cell culture

DC2.4 cells were cultured in RPMI 1640 medium (Gibco) containing 10% foetal bovine serum (FBS, Gibco) and 1% penicillin – streptomycin. Raw264.7 cells and human embryonic lung fibroblast (HELF) cells were cultured in high-glucose Dulbecco's Modified Eagle's Medium (DMEM, Gibco), supplemented with 10% FBS and 1% penicillin – streptomycin. DC2.4 and Raw264.7 cells were subjected to a 48-hour incubation period with 3 μg/mL LPS, 100 μL phosphate buffered saline (PBS), 100 μL inactivated HCMV, and 3 μg/mL RH*Ec*$^{IE1/pp65/pp150}$. Splenic lymphocytes were harvested from mice on day 7 post booster immunization and cultured in RPMI 1640 medium. The cells were cultured for 24 hours with the stimulus and 4 hours with Brefeldin A (Biolegend, cat.420601). Human umbilical vein endothelial cells (HUVECs) were cultured in specialized endothelial cell medium (ECM, ScienCell) containing 5% FBS, 1% endothelial cell growth supplement, and 1% penicillin – streptomycin.

Virus amplification

The laboratory HCMV strain AD169 was amplified in HELF cells. Upon cellular swelling and denaturation, both cells and culture supernatant were collected. The cells underwent three cycles of freeze-thawing at temperatures of −80°C and 37°C, while the supernatant was collected post-centrifugation and filtered through a 0.45 μm filter membrane before storage at −80°C for future use.

HELF cells were seeded at a density of 2×10^5 cells per well in a 96-well plate. The following day, the cells were incubated with serum-free DMEM for 2 hours. The AD169 virus was serially diluted in a 10-fold gradient, resulting in a total of six dilutions. Subsequently, 100 μL of the diluted virus was added to each well and incubated for 2 hours. Following this, the culture medium was discarded, and the 96-well plate was washed with PBS. The cells were then cultured in DMEM supplemented with 2% FBS and 1% penicillin-streptomycin at 37°C with 5% CO_2 for 5–7 days. The $TCID_{50}$ (50% tissue-culture infectious doses) was calculated using the Reed-Muench method [35]. HELF cells not exposed to the virus were utilized as the control group. The titre of HCMV AD169 was determined to be 2.2×10^6 pfu/mL. The formula for calculating $TCID_{50}$ is as follows: $pd = (p1 - 50\%)/(p1 - p2)$, $lgTCID_{50} = lgC + pd \times lgC$ (where $p1$ represents the cytopathic rate exceeding 50%, $p2$ denotes the cytopathic rate below 50%, and C signifies the dilution ratio).

Animal immunization

Female C57BL/6 mice aged 6–8 weeks, purchased from Beijing Vital River, were raised in the SPF Animal Center of Qingdao University according to Institutional Animal Care and Committee guidelines. The mice were randomly assigned to four groups: the blank group (PBS), inactivated HCMV combined with AddaVax group (INA), adjuvant group (AddaVax), and adjuvant combined with recombinant subunit vaccine group (AddaVax + RH*Ec*$^{IE1/pp65/pp150}$), each comprising six mice. Intramuscular injections were administered on days 0 and 28. The AddaVax + RH*Ec*$^{IE1/pp65/pp150}$ group received injections of 50 μL RH*Ec*$^{IE1/pp65/pp150}$ + 50 μL AddaVax. The blank group, AddaVax group, and INA group were injected with equivalent volumes of PBS, AddaVax, and INA (50 μL inactivated HCMV + 50 μL AddaVax), respectively. AddaVax, an oil-in-water nano-emulsion based on squalene, is formulated similarly to MF59, which has been licenced as a vaccine adjuvant [36]. In this study, AddaVax was utilized as an adjuvant in conjunction with RH*Ec*$^{IE1/pp65/pp150}$. The laboratory AD169 strain was inactivated with ultraviolet light for 2 hours to serve as the whole virus control group.

Detection of dendritic cells and macrophages

As mentioned in section 2.2, DC2.4 and Raw264.7 cells were harvested and prepared for cell surface staining. Meanwhile, carry out cell surface marker identification of dendritic cells and macrophages for all lymphocytes in the drained lymph nodes (dLNs) obtained through grinding and filtration. For M1 and M2 macrophages in dLNs, extracellular staining was performed for 30 minutes. The cells were then fixed with 4% paraformaldehyde and 0.2% Triton X-100, followed by intracellular staining with antibodies for 2 hours. Subsequently, the cells were detected using the CytoFLEX. Antibodies were as follows: anti-CD80-PE (Biolegend, cat.104707), anti-CD86-Brilliant Violet 421 (Biolegend, cat.105032), anti-H-2Kb-percp/cy5.5 (Biolegend, cat.116516), anti-I-A/I-E-Alexa Fluor 700 (Biolegend, cat. 107622), anti-CD11b-APC (Biolegend, cat.101212), anti-CD11c-FITC (Biolegend, cat.117306), anti-F4/80-PE/cy7 (Biolegend, cat.123114), anti-CD8a-APC/cy7 (Biolegend, cat.100714), anti-iNOS-PE (Biolegend, cat.696806), and anti-CD206-percp/cy5.5 (Biolegend, cat.141716).

Detection of T cells, memory T cells, and B cells

To identify effector T cells and cytotoxic T cells, spleens were harvested after 7 days of enhanced immunity. GolgiPlug (BD Biosciences) and GolgiStop (BD Biosciences) were added to freshly isolated splenic lymphocytes and peripheral blood mononuclear cells (PBMCs), and then stimulated with RH*Ec*1–1 and RH*Ec*1–2 for 6 hours. Effector T cells and cytotoxic T cells were detected by flow cytometry. The antibodies are as follows: anti-CD3-Pacific Blue, anti-CD8-APC/cy7, anti-CD44-Alexa Fluor 488 (Biolegend, cat.103016), and anti-CD107a-APC (Biolegend, cat.121614). After 140 days of vaccination, memory T cells were stained with anti-CD3-Pacific Blue, anti-CD8-APC/cy7, anti-CD44-Alexa Fluor 488, anti-CD62L-PE/cy7 (Biolegend, cat.104418), anti-CD69-PE /cy7 (Biolegend, cat.104512), and anti-CD103-Alexa Fluor 488 (Biolegend, cat.121408) antibodies. Memory B cells were dyed with anti-CD45R/B220-APC (Biolegend, cat.103212), anti-CD19-FITC (Biolegend, cat.152404), and anti-CD27-PE/cy7 (Biolegend, cat.124216) antibodies. Splenic lymphocytes, as mentioned in section 2.2, were subjected to extracellular staining with antibodies. Afterward, these lymphocytes underwent intracellular staining following pretreatment with paraformaldehyde and Triton X-100. Antibodies were as follows: anti-CD3-Pacific Blue, anti-CD4-Brilliant Violet 605 (Biolegend, cat.100451), anti-CD8-APC/cy7, anti-TNF-α-PE (Biolegend, cat.506306), anti-IFN-γ-PE (Biolegend, cat.505808), anti-IL-2-APC (Biolegend, cat.503810), anti-IL-4-PE (Biolegend, cat.504104), anti-IL-6-APC (Biolegend, cat.504508), and anti-IL-10-PE (Biolegend, cat.505008).

Neutralizing antibody

Neutralizing antibodies against HCMV AD169 strain were assessed in the serum of immunized mice on day 140 using the microneutralization assay described by Nelson et al. [37]. The procedure involved serially diluting mouse serum 2-fold with ECM, starting from an initial dilution of 1:8 and a final dilution of 1:1024. The diluted serum was then mixed with an equal volume of AD169 virus solution at an MOI of 10, followed by incubation at 37°C for 1 hour. Negative controls comprised cells not exposed to the virus, while positive controls included virus-infected cells not incubated with serum.

The treated virus mixture was incubated with HUVECs at 37°C and 5% CO_2 for 48 hours. After fixation and permeabilization of the cells using paraformaldehyde and Triton X-100, they were blocked with BSA for 1 hour. Subsequently, the cells were incubated with a mouse anti-HCMV IE1/2 (1:100, Abcam) monoclonal antibody overnight at 4°C. On the second day, the cells were co-incubated with Cy3-conjugated goat anti-mouse IgG (H + L) (1:500, ABclonal) monoclonal antibodies for 1 hour, followed by DAPI staining of the nucleus for 5 minutes. Neutralization titres (50% inhibitory dilution, ID_{50}) were calculated using Reed and Muench's method [31].

Western blot analysis

We used the ImunoSep Mouse $CD11b^+$ cell positive selection kit (Precision BioMedicals Co., Ltd, China) to isolate $CD11b^+$macrophages from the dLNs of mice 3 days of the initial immunization. Total protein extraction was performed using a total protein extraction kit (Solarbio). After adding the samples, electrophoresis was conducted, followed by membrane transfer and blocking with protein-free rapid blocking buffer (epizyme) for 30 minutes. Primary antibodies were then incubated at 4°C overnight, and the antibodies were as follows: rabbit anti-mouse IKKα (1:500, ABclonal) and rabbit anti-mouse phospho-IKKα (1:500, ABclonal), rabbit anti-mouse IκBα (1:500, ABclonal), rabbit anti-mouse phospho-IκBα (1:500, ABclonal), rabbit anti-mouse NF-κB p65 (1:500, ABclonal), rabbit anti-mouse phospho-NF-κB p65 (1:500, Affinity), and rabbit anti-mouse β-Actin (1:8000, ABclonal). The subsequent day, the membrane was incubated with HRP goat anti-rabbit IgG (H + L) (1:8000, ABclonal)

for 2 hours. Finally, using ECL reagents (Affinity) and chemiluminescence to visualize the proteins.

Statistical analysis

The data obtained from CytoFLEX were processed using FlowJo V10.5.3. All data were analysed using GraphPad Prism 9.5.1, and the results from western blot were processed using Image J. The results are expressed as mean ± SEM (standard error of mean). Statistical analyses involved one-way analysis of variance (ANOVA) and Tukey's test, with differences between groups considered significant for p values < 0.05.

Results

Construction and validation of recombinant subunit vaccine

The protein sequences of HCMV IE1, pp65, and pp150 were obtained from GenBank. The dominant epitopes were predicted using the IEDB and SYFPEITHI databases. IEDB is a database containing vast amounts of immune epitope information, covering various immunological-related data. It collects immune epitope data from multiple species, diseases, and immune types, and provides various tools and resources. SYFPEITHI, on the other hand, is a database with a long-standing accumulation of data, focusing on predicting T cell epitopes. It holds a high level of specialization and reliability in the field of T cell immunology research [27,28]. When predicting antigen epitopes for HCMV IE1, pp65, and pp150 proteins, we included 14 dominant Chinese-restricted alleles (A2, A24, A1, A3, A11, A68, B44, B7, A23, A26, B35, B38, B8, and B27), as well as HLA-DRB1, in our analysis. Epitope sequences with high scores that overlapped between the two databases were screened as T cell candidate epitopes for recombinant vaccines. Those with comprehensive scores exceeding 0.5 in the IEDB database were chosen as B cell candidate epitopes. This approach resulted in the identification of 98 CTL epitopes, 2 Th epitopes, and 7 B cell epitopes. Subsequently, the epitope sequences were concatenated using GGSGGGSGS and divided into two segments for recombination with the pET22b vector. The resulting constructs were then introduced into the *E. coli* expression system to generate recombinant protein vaccines, designated as RH*Ec*-1 and RH*Ec*-2. The RH$Ec^{IE1/pp65/pp150}$ vaccine consists of RH*Ec*-1 and RH*Ec*-2. RH*Ec*-1 consists of 270 amino acids with a molecular weight of approximately 36.7 kDa (Figure 1a), while RH*Ec*-2 comprises 318 amino acids and has a molecular weight of about 41.98 kDa (Figure 1b). We utilized the SWISS-MODEL database to perform a series of rigorous verification tasks, involving evaluating the stereochemical quality of RH*Ec*-1 and RH*Ec*-2 structures, comparing them precisely with homologous proteins of known structures, and conducting energy minimization calculations. These steps ensured the predicted tertiary structures of RH*Ec*-1 and RH*Ec*-2 have high credibility and reasonable quality, providing a solid foundation for further related research (Figure 1c–d).

Safety of recombinant subunit vaccine

To assess the safety of the HCMV recombinant subunit vaccine, we monitored changes in body weight and food intake in mice seven days after enhanced immunization. Additionally, we evaluated serum levels of LDH, CK, ALT, AST, BUN, and CREA to assess potential toxic effects on the heart, liver, and kidney.

The results showed no significant differences in body weight and food intake among the PBS, AddaVax, AddaVax + RH$Ec^{IE1/pp65/pp150}$, and INA

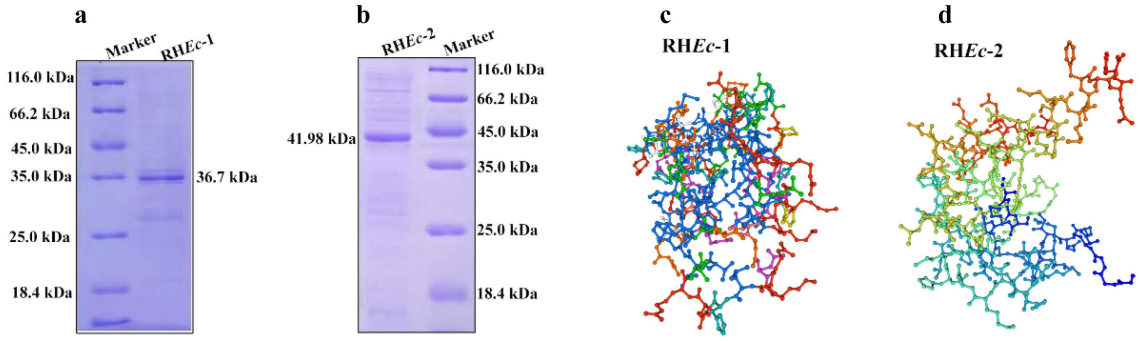

Figure 1. Validation of recombinant subunit vaccines. (a–b) Ultrasonic fragmentation of recombinant *E. coli*, taking the supernatant to detect protein, after SDS-polyacrylamide gel electrophoresis, using Coomassie brilliant blue detection. (c–d) The SWISS-MODEL database was used to predict the three-dimensional structure of RH*Ec*-1 and RH*Ec*-2.

groups (Figure 2a–b). Serum levels of cardiac indicators (LDH and CK), liver indexes (ALT and AST), and renal indicators (BUN and CREA) were within normal ranges. Although ALT and BUN levels in the AddaVax + RH*Ec*$^{IE1/pp65/pp150}$ group were slightly lower than in the PBS group, they remained within the normal range, and the changes were not clinically significant (Figure 2c–h). Therefore, the recombinant HCMV vaccine RH*Ec*$^{IE1/pp65/pp150}$ was safe in mice and did not exhibit any obvious toxic effects on the heart, liver, and kidney.

The recombinant subunit vaccine activates DC2.4 and Raw264.7 cells in vitro

To assess the ability of the recombinant subunit vaccine to activate antigen-presenting cells (APCs) in *vitro*, DC2.4 and Raw264.7 cells were stimulated with 3 μg/mL RH*Ec*$^{IE1/pp65/pp150}$ for 48 hours. The expression of costimulatory molecules on the cell surface was then detected using flow cytometry, with LPS serving as the positive control and PBS as the negative control.

The results demonstrated that RH*Ec*$^{IE1/pp65/pp150}$ induced a significant upregulation of CD80, CD86, CD40, and MHCII expression on the surface of DC2.4 and Raw264.7 cells. In DC2.4 cells, the percentage of CD40 even exceeded 80%, representing a 6.1-fold increase compared to the PBS group. CD80, CD86, CD40, and MHCII expression in the RH*Ec*$^{IE1/pp65/pp150}$ group were significantly higher than those in the other groups ($p < 0.01$) (Figure 3a–b and Figure S1a). In Raw264.7 cells, the expression of CD80 and CD86 increased significantly, showing a 3.5-fold and 6.3-fold increase compared to the PBS group, respectively ($p < 0.0001$). Compared with the LPS, PBS, and inactivated HCMV groups, the RH*Ec*$^{IE1/pp65/pp150}$ group showed the most significant upregulation of CD80, CD86, CD40, and MHCII percentages ($p < 0.0001$) (Figure 3c–d and Figure S1b). Therefore, RH*Ec*$^{IE1/pp65/pp150}$ efficiently activates APCs in *vitro* and induces their phenotypic maturation.

The RHEc$^{IE1/pp65/pp150}$ activates DCs and macrophages in vivo

To evaluate the ability of the recombinant HCMV subunit vaccine RH*Ec*$^{IE1/pp65/pp150}$ to activate APCs in *vivo*, we examined the expression of costimulatory molecules on the surface of APCs in mouse dLNs one day after immunizing mice with PBS, AddaVax, AddaVax + RH*Ec*$^{IE1/pp65/pp150}$, and INA. The results demonstrated that the expressions of CD80, CD86, MHCI, and MHCII on the surface of CD11c^{+} dendritic cells after RH*Ec*$^{IE1/pp65/pp150}$ immunization were

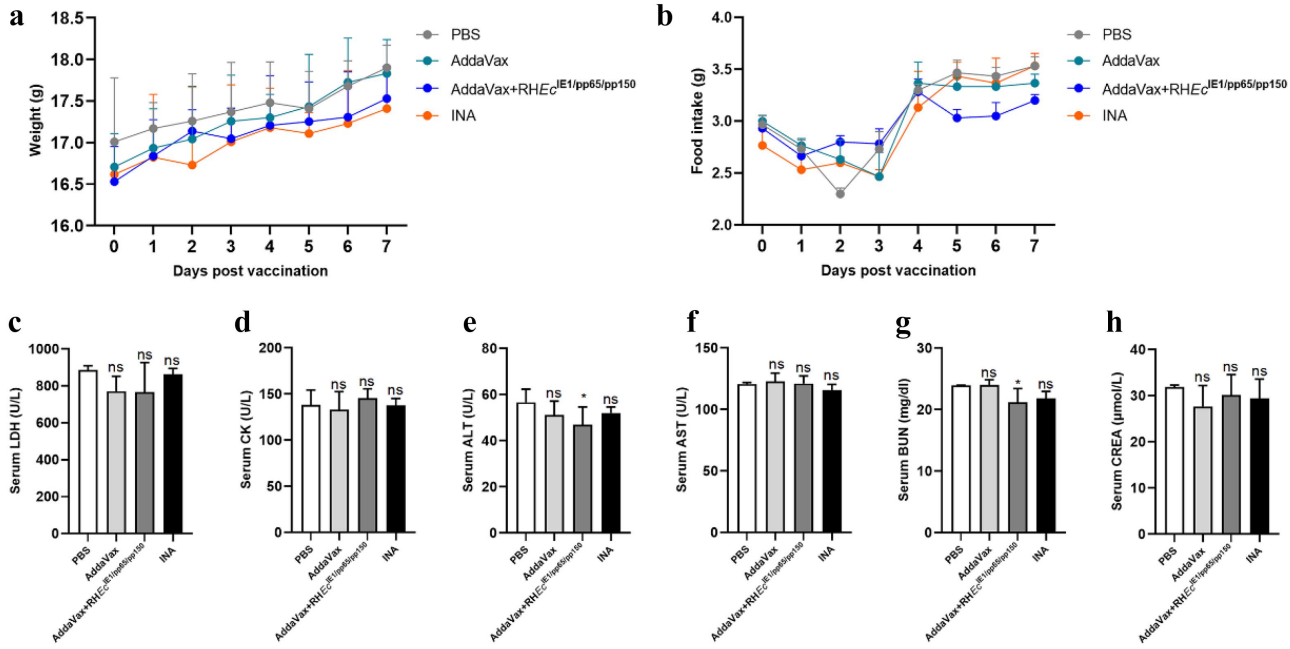

Figure 2. Safety of RH*Ec*$^{IE1/pp65/pp150}$ vaccine. (a–b) Changes in body weight and food intake in mice within seven days after enhanced immunization. (c–h) After seven days of enhanced immunity, the levels of serum lactate dehydrogenase (LDH), creatine kinase (CK), Alanine aminotransferase (ALT), aspartate aminotransferase (AST), blood urea nitrogen (BUN), and creatinine (CREA) in mice were measured using an automatic biochemical analyzer according to the reagent instructions. Six mice in each group. One-way ANOVA was used for statistical analysis. The results were expressed as mean ± SEM, $^{*}p < 0.05$.

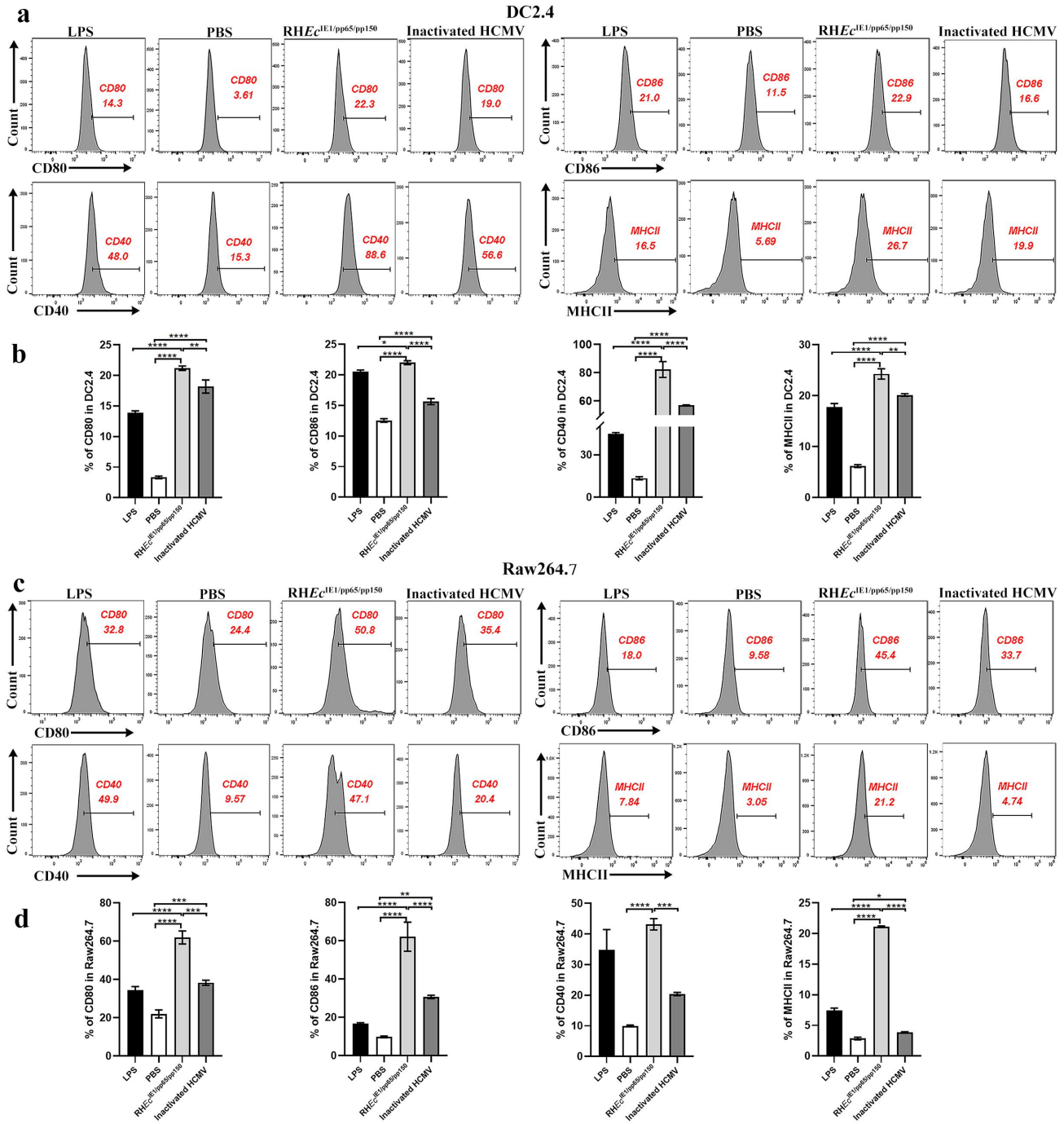

Figure 3. The RH*Ec*$^{IE1/pp65/pp150}$ vaccine activates APCs in *vitro*. DC2.4 and Raw264.7 cells were stimulated with LPS, PBS, RH*Ec*$^{IE1/pp65/pp150}$, and inactivated HCMV for 48 hours. (a–d) Flow cytometry was used to detect the surface costimulatory molecules CD80, CD86, CD40, and MHCII in DC2.4 and Raw264.7 cells. All experiments were repeated at least 3 times, using one-way ANOVA and Tukey's test, bars represent mean ± SEM, and differences were indicated by asterisks *$p < 0.05$, **$p < 0.01$, ***$p < 0.001$, and ****$p < 0.0001$.

significantly upregulated, reaching 8.26%, 13.8%, 9.68%, and 4.7%, respectively, compared to other groups. Particularly, the expressions of CD86, MHCI, and MHCII were higher than those in the INA group ($p < 0.01$) (Figure 4a and Figure S2a – b). Similarly, the percentages of CD80, CD86, MHCI, and MHCII on the surface of CD11b^{+} macrophages in the AddaVax + RH*Ec*$^{IE1/pp65/pp150}$ group were 9.13%, 82.0%, 10.9%, and 3.82%, respectively, showing significant differences from other groups ($p < 0.0001$). Notably, the proportion of CD86 in the AddaVax + RH*Ec*$^{IE1/pp65/pp150}$ group reached 82%, representing a 4.3-fold increase compared to the INA group ($p < 0.0001$) (Figure 4b and Figure S2c–d). Therefore, the

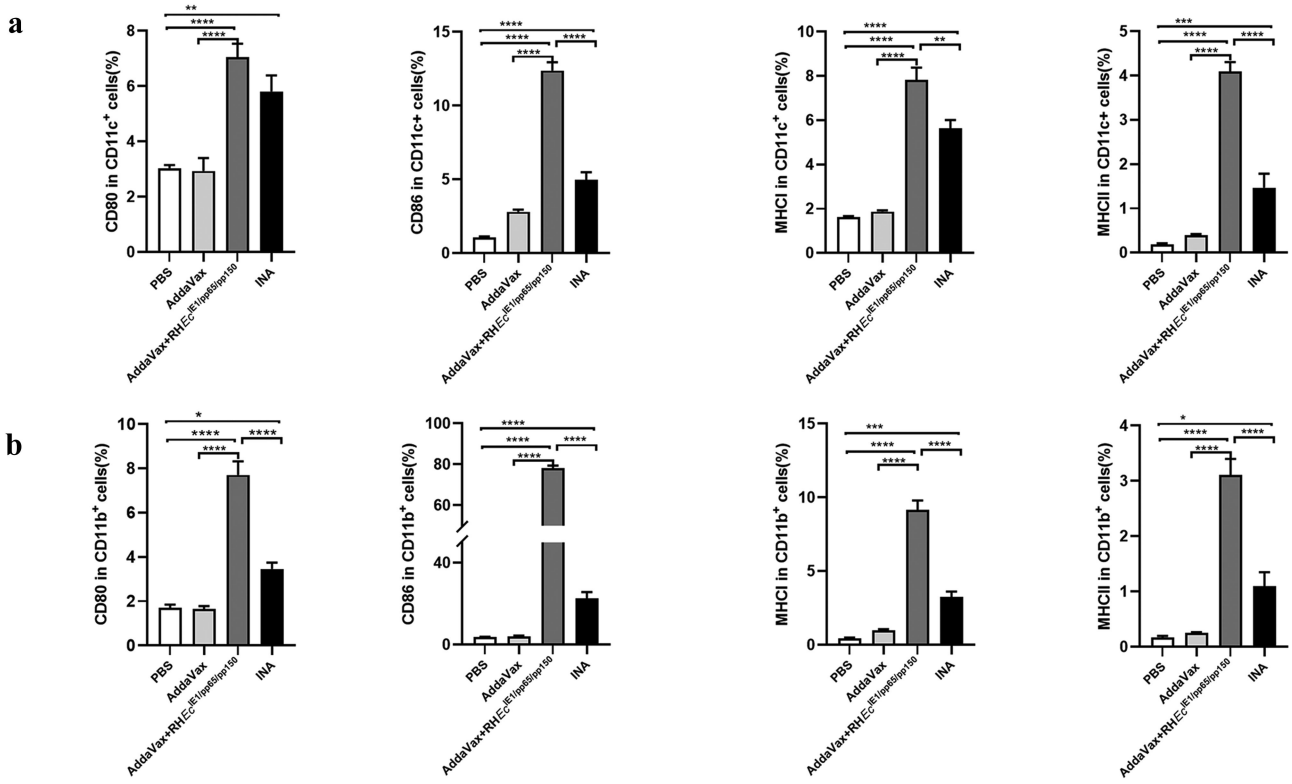

Figure 4. The RH*Ec*$^{IE1/pp65/pp150}$ vaccine activates APCs in *vivo*. (a–b) Female C57BL/6 mice aged 6–8 weeks were immunized with PBS, AddaVax, AddaVax+RH*Ec*$^{IE1/pp65/pp150}$, and INA for one day. Flow cytometry was used to detect the expression of co-stimulated molecules on the surface of $CD11c^+$ dendritic cells and $CD11b^+$ macrophages in the dLns. Six mice in each group were analyzed by one-way ANOVA and Tukey's test. Results were expressed as mean ±SEM and differences were indicated by asterisk $*p < 0.05$, $**p < 0.01$, $***p < 0.001$, and $****p < 0.0001$.

RH*Ec*$^{IE1/pp65/pp150}$ vaccine promoted the phenotypic maturation of APCs in *vivo*.

The RHEc$^{IE1/pp65/pp150}$ vaccine induced innate immune responses via NF-κB pathway

Immature dendritic cells (DCs) capture antigens from peripheral tissues and activate other maturing DCs, upregulating costimulatory molecules, including CD80, CD86, CD40, and MHC, facilitating efficient migration to draining lymph nodes for antigen presentation to T cells [38,39]. Our results indicate that RH*Ec*$^{IE1/pp65/pp150}$ distinctly activates phenotypic maturation of APCs in *vitro* and in *vivo*.

To further characterize the innate immune response induced by RH*Ec*$^{IE1/pp65/pp150}$, we analysed the dLNs of mice three days after the initial immunization using flow cytometry [40,41]. In comparison to the PBS and AddaVax groups, the percentage of migratory DCs ($CD11c^+MHCII^{hi}$), resident DCs ($CD11c^+MHCII^+$), $CD8a^+$rDCs ($CD11c^+MHCII^+CD8a^+$), and $CD11b^+$rDCs ($CD11c^+MHCII^+CD11b^+$) in the AddaVax + RH*Ec*$^{IE1/pp65/pp150}$ group significantly increased ($p < 0.01$). Previous reports have classified macrophages into M1 and M2 types, where M1 macrophages mediate pro-inflammatory responses, Th1 immune responses, antigen presentation, and pathogen killing, while M2 macrophages primarily mediate Th2-type immune regulation [42,43]. Similar to dendritic cells, M1 ($CD11b^+F4/80^+iNOS^+$) and M2 ($CD11b^+F4/80^+CD206^+$) macrophages in the AddaVax + RH*Ec*$^{IE1/pp65/pp150}$ group showed a significant increase compared to the PBS and AddaVax groups ($p < 0.05$) (Figure 5a–c).

The findings illustrated that the RH*Ec*$^{IE1/pp65/pp150}$ vaccine significantly induced the phenotypic maturation of APCs both in *vitro* and in *vivo*. Moreover, it markedly enhanced the migration of dendritic cell subsets and macrophage subsets to dLNs. To examine whether the RH*Ec*$^{IE1/pp65/pp150}$ vaccine triggers innate immune responses, we isolated $CD11b^+$ macrophages from dLNs of mice three days post-initial immunization with the vaccine, and assessed the downstream proteins of the Toll-like receptor signalling pathway

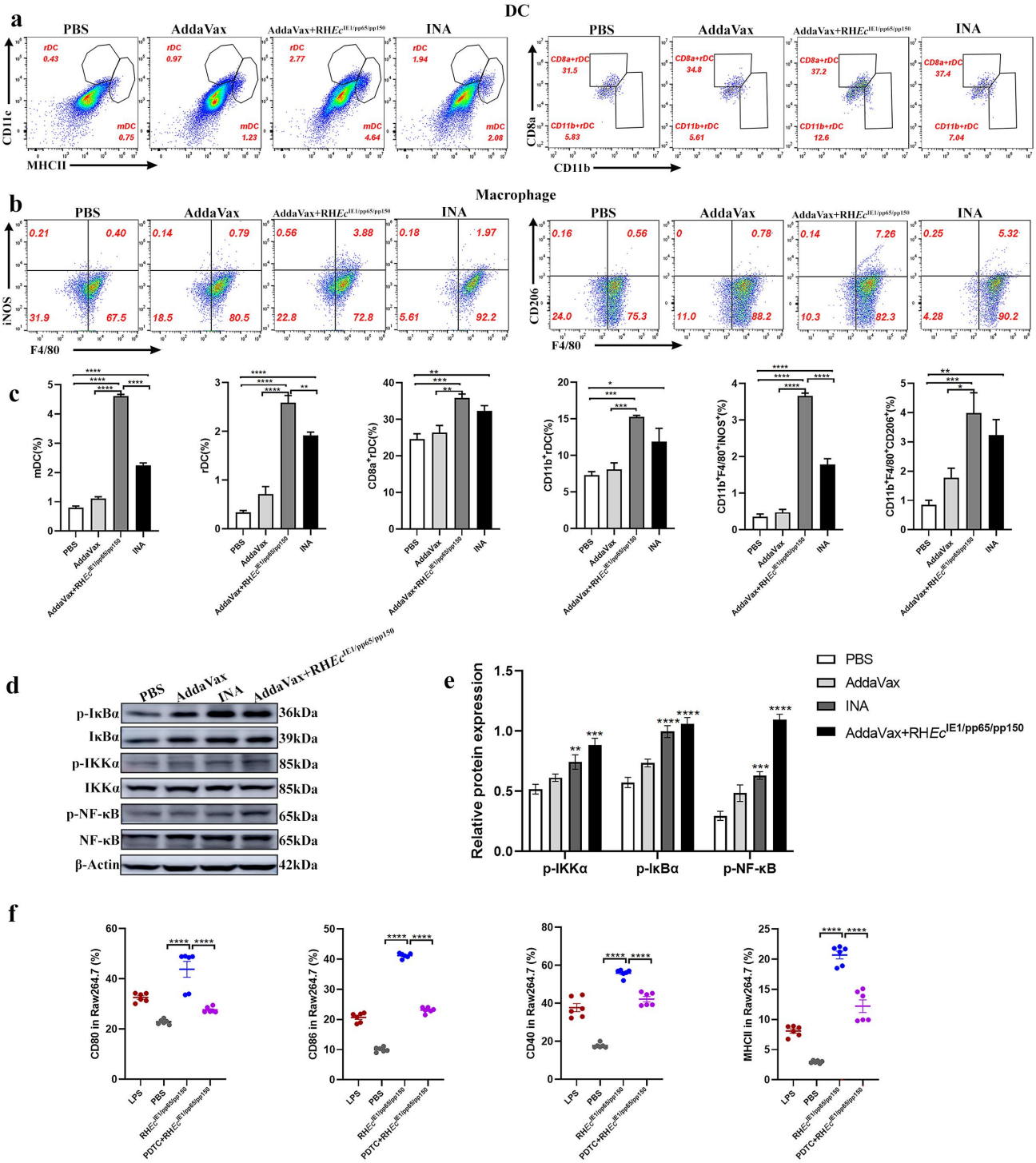

Figure 5. The RH*Ec*$^{IE1/pp65/pp150}$ induces innate immune responses in draining lymph nodes. (a–c) After three days of initial immunization, flow cytometry was used to detect mDcs, rDcs, CD8a$^+$rDCs, CD11b$^+$rDCs, M1, and M2 macrophages in the dLns. (d–e) Three days after the initial immunization, CD11b$^+$ macrophages were isolated from the dLNs of mice and total protein was extracted. Then, western blotting was employed to detect proteins associated with the NF-κB pathway. (f) Raw264.7264.7 cells were pretreated with 20 μM PDTC for 1 hour and co-cultured with RH*Ec*$^{IE1/pp65/pp150}$ for 48 hours. CD80, CD86, CD40, and MHCII were detected using flow cytometry. Six mice in each group, using one-way ANOVA and Tukey's test. All experiments were repeated at least three times. The results were obtained using mean ± SEM, with differences indicated by asterisks *$p < 0.05$, **$p < 0.01$, ***$p < 0.001$, and ****$p < 0.0001$.

using western blotting. Fortunately, we found that compared to PBS, AddaVax, and INA groups, key proteins in the NF-κB signalling pathway, including phosphorylated IKKα (p-IKKα), p-IκBα, and p-NF-κB, were significantly upregulated in the AddaVax + RH*Ec*$^{IE1/pp65/pp150}$ group (Figure 5d–e).

To further validate that the RH*Ec*$^{IE1/pp65/pp150}$ vaccine induces macrophage maturation via the NF-κB pathway, we pretreated Raw264.7 cells with 20 μM PDTC (NF-κB inhibitor) for 1 hour and then co-cultured them with RH*Ec*$^{IE1/pp65/pp150}$ for 48 hours to assess the expressions of CD80, CD86, CD40, and MHCII. However, when compared with the RH*Ec*$^{IE1/pp65/pp150}$ group, the expressions of CD80, CD86, CD40, and MHCII in the PDTC + RH*Ec*$^{IE1/pp65/pp150}$ group significantly decreased after treatment with the NF-κB inhibitor ($p < 0.0001$) (Figure 5f). Therefore, the RH*Ec*$^{IE1/pp65/pp150}$ vaccine may activate the innate immune response via the NF-κB pathway.

Recombinant subunit vaccine RHEc$^{IE1/pp65/pp150}$ induces T-cell response

As previously mentioned, RH*Ec*$^{IE1/pp65/pp150}$ activated DCs and macrophages, acting as a bridge between innate and adaptive immune responses. Subsequently, we evaluated the splenic T-cell response in mice seven days after immune enhancement (Figure 6a). We examined the secretion of tumour necrosis factor-α (TNF-α), interferon-γ (IFN-γ), interleukin-2 (IL-2) secreted by $CD8^+$ T cells, as well as TNF-α, IFN-γ, IL-2, IL-4, IL-6, and IL-10 by $CD4^+$T cells. $CD8^+$T cells in the AddaVax + RH*Ec*$^{IE1/pp65/pp150}$ group generated a large amount of TNF-α, IFN-γ, and IL-2. Moreover, in the AddaVax + RH*Ec*$^{IE1/pp65/pp150}$ group, there was a significant increase in the proportion of effector T cells ($CD3^+CD8^+CD44^+$) and cytotoxic T cells ($CD3^+CD8^+CD107a^+$) ($p < 0.001$) (Figure 6b–d).

Additionally, the proportions of $CD4^+$TNF-α^+T cells, $CD4^+$IFN-γ^+T cells, and $CD4^+$IL-2^+T cells in the AddaVax + RH*Ec*$^{IE1/pp65/pp150}$ group were 13.5%, 26.3%, and 9.6%, respectively, significantly higher than those in the PBS, AddaVax, and INA groups ($p < 0.0001$). The levels of IL-4, IL-6, and IL-10 secreted by $CD4^+$T cells in the AddaVax + RH*Ec*$^{IE1/pp65/pp150}$ group were also significantly higher than those in other groups, even surpassing those in the INA group ($p < 0.01$) (Figure 6e–f). In summary, the RH*Ec*$^{IE1/pp65/pp150}$ vaccine induced abundant effector T cells, cytotoxic T cells, and activated T cells to secrete various cytokines.

The RHEc$^{IE1/pp65/pp150}$ vaccine induces memory cell proliferation

Memory T and B cells, originating from naïve cells clonally expanded during the immune response, persist after the elimination of antigens. These memory cells generate a more timely and robust response upon re-exposure to antigens, contributing to the individual's ability to clear pathogens [44]. In this study, we monitored memory B cells ($B220^+CD19^+CD27^+$), effector memory T cells (T_{EM}: $CD3^+CD8^+CD44^+CD62L^{lo}$), central memory T cells (T_{CM}: $CD3^+CD8^+CD44^+CD62L^{hi}$), and tissue-resident memory T cells (T_{RM}: $CD3^+CD8^+CD69^+CD103^+$) in mouse bone marrow and peripheral tissues 140 days after immunizations (Figure 7a–c). The results revealed a significant increase in memory B cells in the bone marrow and peripheral tissues of the AddaVax + RH*Ec*$^{IE1/pp65/pp150}$ group compared to the PBS, AddaVax, and INA groups ($p < 0.01$) (Figure 7d). Compared with the other groups, the neutralizing antibody titre in the AddaVax + RH*Ec*$^{IE1/pp65/pp150}$ group was markedly higher, reaching a titre of 256 on day 140 after immunizations (Figure 7e). Additionally, the percentages of T_{EM}, $T_{RM,}$ and memory B cells in the spleen and lymph nodes were significantly higher than those in the INA group ($p < 0.001$). Notably, T_{CM} showed a substantial increase in spleen, lymph nodes, and bone marrow of the AddaVax + RH*Ec*$^{IE1/pp65/pp150}$ group ($p < 0.01$), but not in peripheral blood (Figure 7f–h). In conclusion, the RH*Ec*$^{IE1/pp65/pp150}$ vaccine effectively induces robust proliferation of memory cells and neutralizing antibodies in mice.

Discussion

HCMV is widespread worldwide and possesses the largest known human virus genome (around 235 kbp). HCMV infection causes latent, lifelong infection in multiple host cells mediated by distinct entry mechanisms [11]. HCMV infection causes a considerable risk of morbidity and mortality among immunosuppressed patients, making HCMV-related diseases an important medical problem [5,45]. Existing antiviral drugs have many limitations, including toxicity drug interactions, and antiviral resistance. There is an urgent need to develop safe and effective CMV therapies to avoid the adverse effects associated with small molecule antiviral inhibitors [46,47]. The natural infection of HCMV fails to effectively expose dominant antigenic epitopes, and HCMV successfully evades host immune responses through various

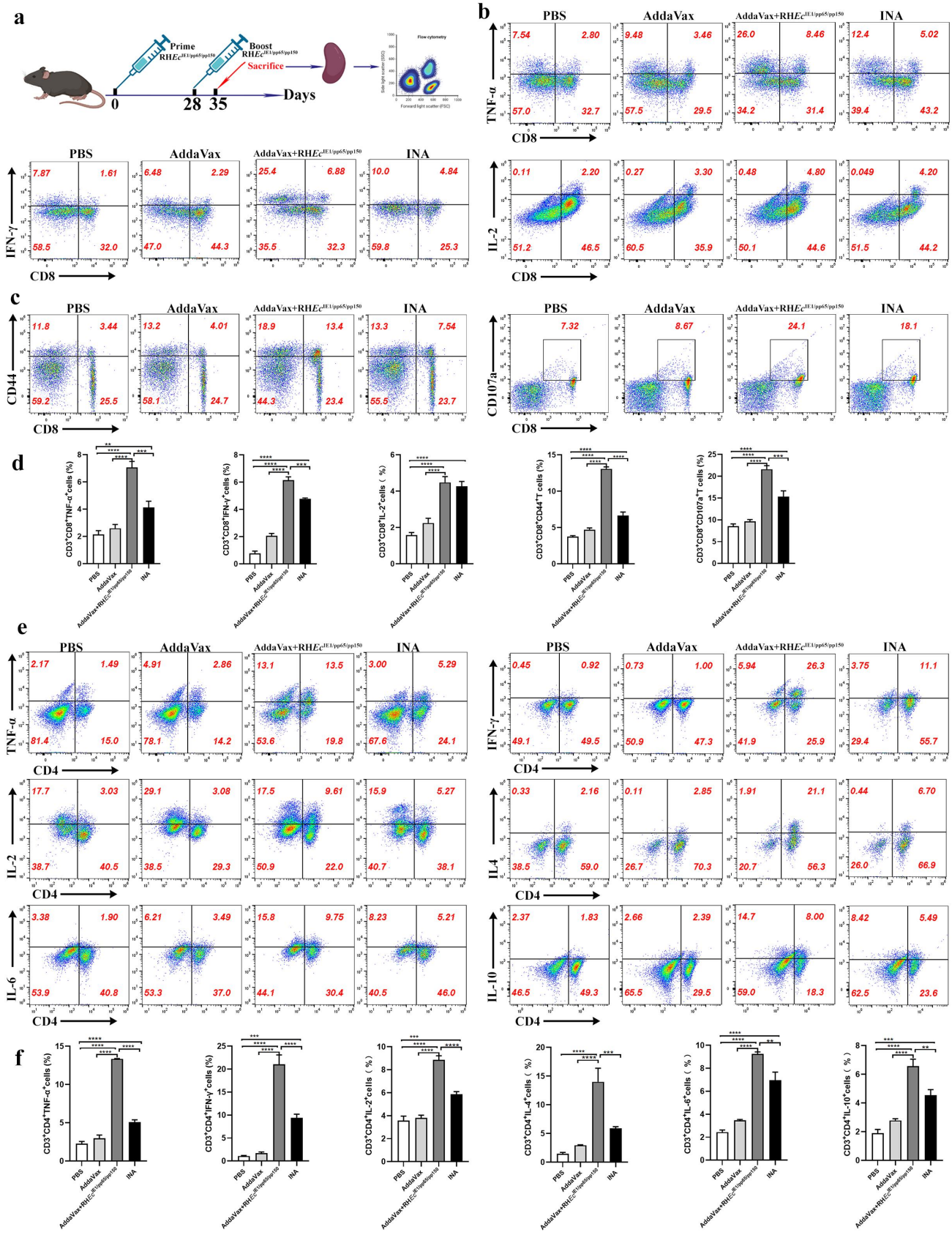

Figure 6. The RH*Ec*$^{lE1/pp65/pp150}$ vaccine induces T-cell responses. (a) Experimental design. (b–f) Seven days after the booster, flow cytometry was used to detect cytokine secretion, effector T cells, and cytotoxic T cells in splenic lymphocytes. Six mice per group were analyzed using one-way ANOVA and Tukey's test. The results were obtained using mean ± SEM, with differences indicated by asterisks *$p < 0.05$, **$p < 0.01$, ***$p < 0.001$, and ****$p < 0.0001$.

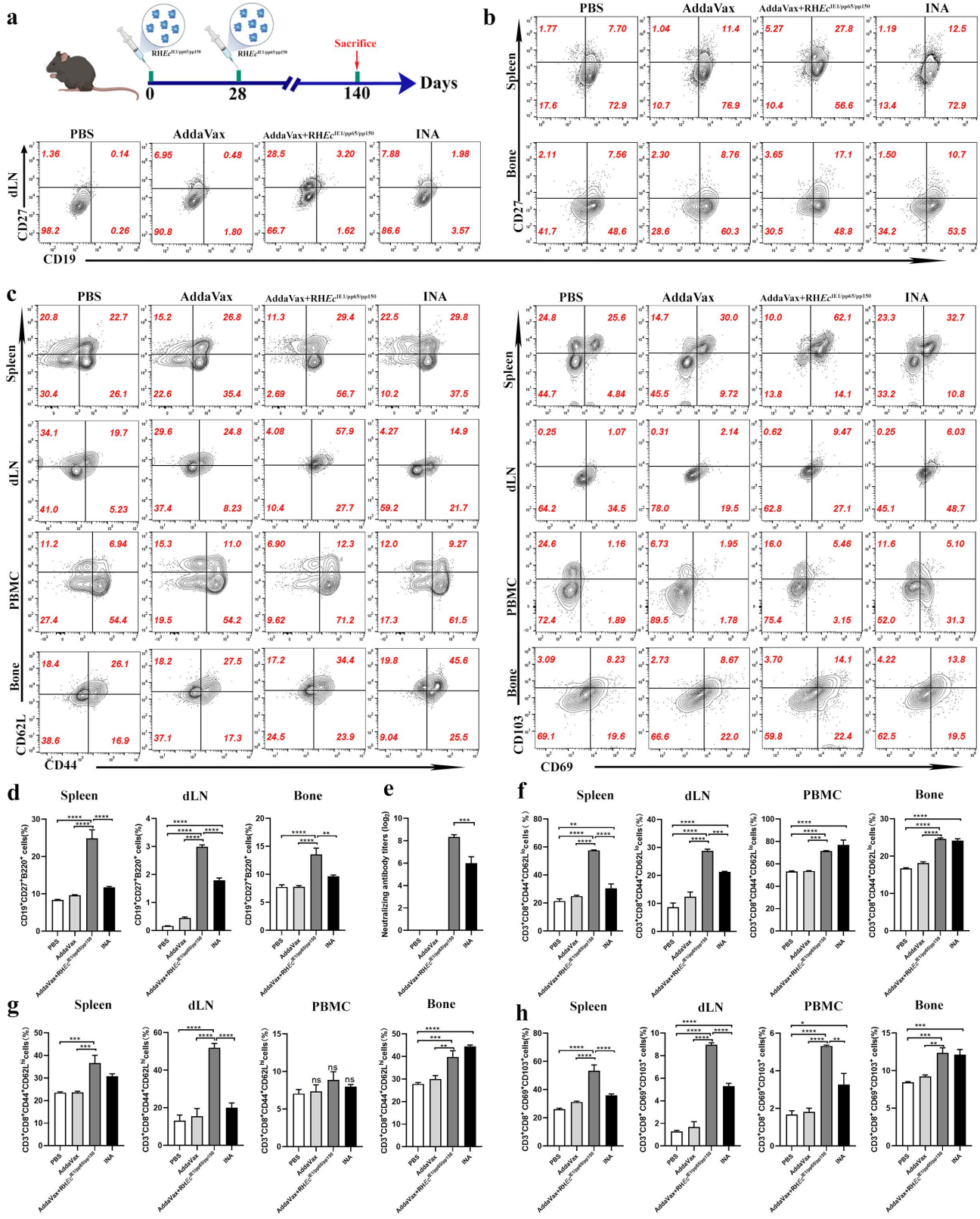

Figure 7. The RH*Ec*$^{IE1/pp65/pp150}$ vaccine induces memory cells and neutralizing antibody production. (a) Immunization protocol and timeline. (b–c) Flow cytometry was used to monitor the memory cells in central and peripheral tissues after 140 days immunization. (d) Statistical results of memory B cells in bone marrow and peripheral tissues. (e) Detection of neutralizing antibody titers in mouse serum. (f–h) Statistical results of T_{EM}, T_{CM}, and T_{RM} in bone marrow and peripheral tissues. One-way ANOVA and Tukey's test were performed. Six mice per group. Bars represented mean ± SEM, *$p < 0.05$, **$p < 0.01$, ***$p < 0.001$, and ****$p < 0.0001$.

mechanisms. Consequently, T and B-cell epitope vaccines have been explored for the development of HCMV vaccines and show promising prospects [12,31].

Recently, immunoinformatics methods have been successfully used in the development of vaccines for various diseases due to their high efficiency, rapidity, and accuracy [48,49]. We applied immunoinformatics tools such as IEDB and SYFPEITHI, to screen the dominant epitopes of abundant CTL, Th, and B cells in the major HCMV proteins pp65, pp150, and IE1. To elicit robust immune responses, we selected epitopes from overlapping regions of the two databases with high scores. We linked the peptide epitopes with GGSGGGSGS and expressed them in *E. coli* as a recombinant protein vaccine.

Compared with complete pathogens, recombinant proteins are easier to synthesize, cause fewer toxic side effects, and can efficiently expose antigen epitopes. Safety, with no obvious toxic side effects, is a primary criterion for a successful vaccine should possess. Therefore, we first evaluated the safety of the vaccine. We observed no significant weight loss or anorexia in the mice after injection of the vaccine, and changes in cardiac, liver, and kidney biochemical indexes were within normal ranges in all groups (Figure 2).

A key aspect of the vaccine strategy is to ensure effective recognition and uptake by APCs such as DCs and macrophages [42]. In this study, both in *vitro* and in *vivo* results indicated that the RH*Ec*$^{IE1/pp65/pp150}$ vaccine can effectively induce the expression of CD80, CD86, MHCI, and MHCII on the surface of APCs, providing sufficient evidence for the phenotypic maturation of APCs (Figures 3 and 4). In *vivo*, APCs bridge innate and adaptive immunity, and mature DCs migrate to secondary lymph nodes, presenting antigens to T cells and stimulating adaptive immunity. Three days after immunization with the RH*Ec*$^{IE1/pp65/pp150}$ vaccine, the numbers of mDC, rDC, CD8^{+}rDC, and CD11b^{+}rDC increased significantly (Figure 5a–c). We explored the underlying mechanism of innate immune activation and found a significant increase in p-IKKα, p-IκBα, and p-NF-κB in the AddaVax + RH*Ec*$^{IE1/pp65/pp150}$ group. After pretreating macrophages with NF-κB inhibitors in *vitro*, we observed substantial reductions in CD80, CD86, MHCI, and MHCII, further confirming that the RH*Ec*$^{IE1/pp65/pp150}$ vaccine can activate the innate immune response via the NF-κB pathway (Figures 5 and 8).

We demonstrated that administering the RH*Ec*$^{IE1/pp65/pp150}$ vaccine resulted in a prominent programmed activation of innate immunity. While this immediate response is crucial, a successful HCMV vaccine also needs to induce adaptive immunity, which must be maintained as immune memory. Studies have reported that the T lymphocyte-mediated cellular responses, including CD4^{+} and CD8^{+} T cell-mediated antiviral functionalities, can potently suppress viral replication and protect against severe disease following HCMV infection [47,50–53].

We found a significant increase in effector T cells and cytotoxic T cells in mice after immunization with

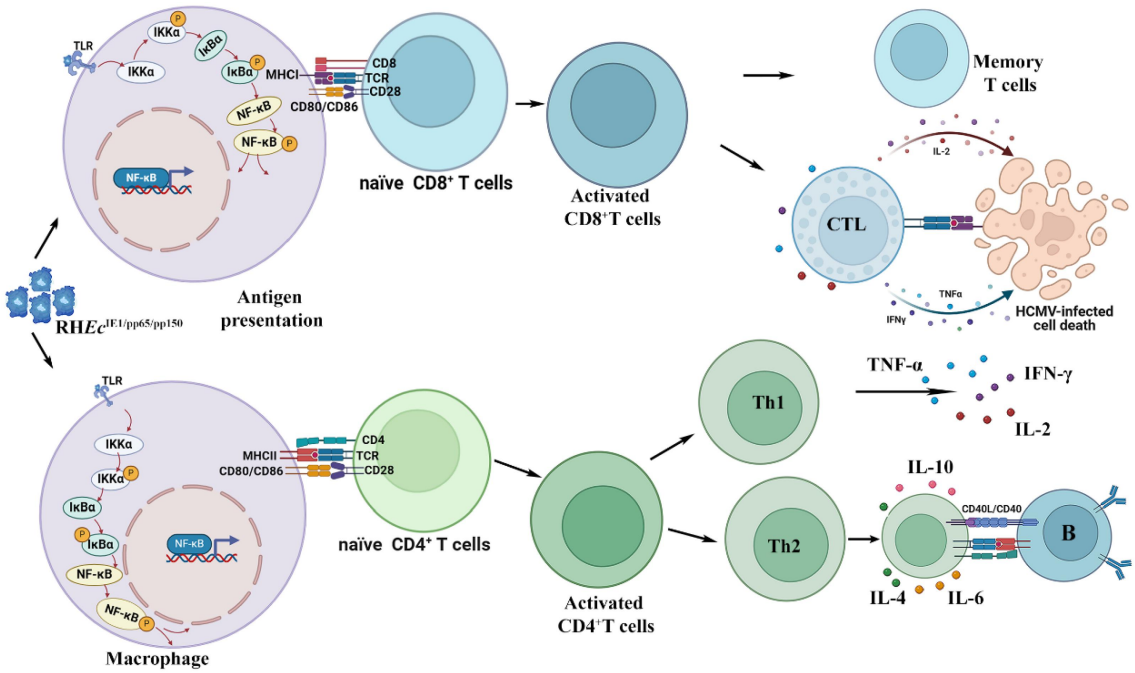

Figure 8. Schematic diagram of RH*Ec*$^{IE1/pp65/pp150}$ vaccine activating innate and adaptive immunity.

the RH*Ec*$^{IE1/pp65/pp150}$ vaccine. Similar to previous studies, the vaccine effectively activated $CD8^+$T cells to secrete abundant TNF-α, IFN-γ, and IL-2. Moreover, the RH*Ec*$^{IE1/pp65/pp150}$ vaccine induced higher expression of TNF-α, IFN-γ, and IL-2 in $CD8^+$T cells, promoting an adaptive immune bias towards Th1. $CD4^+$T cells also secrete large amounts of IL-4, IL-6, and IL-10, which may facilitate the activation of B cells to initiate humoral immune responses against HCMV infection (Figures 6 and 8). In addition, IFN-γ and IL-10 have also been shown to be associated with inhibition of HCMV infection and reactivation [54–57].

Recent studies on immune memory in mice and humans have highlighted the critical role of memory B cells in preventing recurrent viral infections, particularly those caused by variant viruses [58]. Two important types of memory T cells, namely T_{EM} with high cytotoxicity and T_{CM} cells with high proliferation capacity, are important for preventing HCMV reinfection [50,59]. T_{RM} exhibits superior immunity to local challenges compared to circulating memory cells, as they are strategically locates at sites of pathogen entry and reactivation [60]. Hunter K Roark et al. reported that triggering neutralizing antibodies against HCMV as a fundamental feature in effective vaccine development [61]. Consistent with previous research, we found that the RH*Ec*$^{IE1/pp65/pp150}$ vaccine can stimulate the generation of high levels of memory B cells, neutralizing antibodies, T_{EM}, T_{CM}, and T_{RM}, contributing to resistance against viral infections. Even after 140 days of immunization, memory cells remained at a high level with T_{EM}, T_{RM}, and memory B cells particularly prominent in the spleen and dLNs. Remarkably, these levels were significantly higher than those observed in the complete pathogen INA group, suggesting that the RH*Ec*$^{IE1/pp65/pp150}$ vaccine-induced immune response may have a long-term protective effect against HCMV recurrence and reinfection (Figures 7 and 8).

Our vaccine has shown a prominent response in mice, however, there are undeniably limitations. HCMV infection is highly species-specific, which restricts its use in experimental animals. This limitation is a significant reason for the absence of viral challenges in this study. Developing animal models for HCMV virus infection has always posed a substantial challenge in HCMV vaccine development. Moreover, due to the limited blood and tissue specimens collected from mice, we only evaluated the total memory cell pool. Full epitope-specific mapping of T cell responses in the future will add the important detailed resolution of HCMV-specific T cell. Our experiments reflect the superior immune efficacy of the recombinant HCMV protein vaccine to a certain extent, they do not fully represent the effects in the broader population.

Research has reported that HCMV is closely related to the CMVs of nonhuman primates [61]. Therefore, our future research will be further validated in humanized mouse models or nonhuman primates. Nevertheless, we have successfully screened efficacious T and B-cell epitopes using immunoinformatics software and developed a new candidate vaccine for HCMV. Our findings confirm that this recombinant subunit vaccine can programmatically activate innate and adaptive immunity, exerting long-term protective effects, providing novel ideas and perspectives for the development and design of ideal HCMV vaccines.

Acknowledgements

Authors would like to acknowledge language service company (https://www.enago.cn/), reagent companies, and foundations.

Disclosure statement

No potential conflict of interest was reported by the author(s).

Funding

This work was supported by the National Key Research and Development Program of China under Grant [2018YFA0900802]; Shandong Provincial Science and Technology Foundation under Grant [2019JZZY011009]; Qingdao Municipal Science and Technology Foundation under Grant [20-2-3-4-nsh]; and Shandong Provincial Natural Science Foundation under Grant [ZR2021QH254].

ARRIVE guidelines

The study adhered to the ARRIVE guidelines and uploaded a complete checklist.

Author contributions

Zonghui Li: Conceptualization, Writing-original manuscript, Investigation, Software and Data analysis. Shasha Jiang: Data collation, Software analysis, and Writing-manuscript. Fengjun Liu: Methodology and Conceptualization. Xiaoli Yang and Wenxuan Liu: Investigation, Conceptualization, and Validation. Xu Li, Jun Li and Meng Yu: Investigation, Methodology, and Conceptualization. Zhun Wei: Methodology, Software and Validation. Bin Wang and Dongmeng Qian: Conceptualization, Funding acquisition, Resources, Supervision, Writing-review, and Editing. All authors have read and agreed to the published version of the manuscript.

Data availability statement

Data stored in the supplementary materials and repository figshare (http://doi.org/10.6084/m9.figshare.27203523).

Ethics approval and consent to participate

Animal experiments were conducted in accordance with the guidelines of the Animal Welfare and Research Ethics Committee of Qingdao University (Approval ID: No.20220928C5716820230223119).

ORCID

Zonghui Li http://orcid.org/0009-0001-7593-5279
Shasha Jiang http://orcid.org/0000-0003-1102-6401
Bin Wang http://orcid.org/0000-0002-8708-036X
Dongmeng Qian http://orcid.org/0009-0009-1074-1607

References

[1] Griffiths P and Reeves M. Pathogenesis of human cytomegalovirus in the immunocompromised host. Nat Rev Microbiol. 2021;19(12):759–773. doi: 10.1038/s41579-021-00582-z
[2] Zuhair M, Smit GSA, Wallis G, et al. Estimation of the worldwide seroprevalence of cytomegalovirus: a systematic review and meta-analysis. Rev Med Virol. 2019;29(3):e2034. doi: 10.1002/rmv.2034
[3] Atabani SF, Smith C, Atkinson C, et al. Cytomegalovirus replication kinetics in solid organ transplant recipients managed by preemptive therapy. Am J Transplant. 2012;12(9):2457–2464. doi: 10.1111/j.1600-6143.2012.04087.x
[4] Staras SA, Flanders WD, Dollard SC, et al. Influence of sexual activity on cytomegalovirus seroprevalence in the United States, 1988–1994. Sex Transm Dis. 2008;35(5):472–479. doi: 10.1097/OLQ.0b013e3181644b70
[5] Crawford LB, Diggins NL, Caposio P, et al. Advances in model systems for human cytomegalovirus latency and reactivation. MBio. 2022;13(1):e0172421. doi: 10.1128/mbio.01724-21
[6] Karen B, Fowler SS, Robert F. Pass, maternal immunity and prevention of congenital cytomegalovirus infection. JAMA. 2003;289(8):1008–1011. doi: 10.1001/jama.289.8.1008
[7] Karen B, Fowler AJD, Suresh B, et al. Pass, newborn hearing screening: will children with hearing loss caused by congenital cytomegalovirus infection be missed? J Pediatr. 1999;135(1):60–64. doi: 10.1016/S0022-3476(99)70328-8
[8] Kenneson A, Cannon MJ. Review and meta-analysis of the epidemiology of congenital cytomegalovirus (CMV) infection. Rev Med Virol. 2007;17(4):253–276. doi: 10.1002/rmv.535
[9] Neuber S, Wagner K, Goldner T, et al. Mutual interplay between the human cytomegalovirus Terminase subunits pUL51, pUL56, and pUL89 promotes Terminase complex formation. J Virol. 2017;91(12):e02384–16. doi: 10.1128/JVI.02384-16
[10] Härter G, Michel D. Antiviral treatment of cytomegalovirus infection: an update. Expert Opin Pharmacother. 2012;13(5):623–627. doi: 10.1517/14656566.2012.658775
[11] Ligat G, Alain S, Hantz S. Towards a prophylactic vaccine for the prevention of HCMV infection. Vaccines (Basel). 2021;9(9):968. doi: 10.3390/vaccines9090968
[12] Zhang S, Nan F, Jiang S, et al. CRM197-conjugated peptides vaccine of HCMV pp65 and gH induce maturation of DC and effective viral-specific T cell responses. Virulence. 2023;14(1):2169488. doi: 10.1080/21505594.2023.2169488
[13] Link EK, Brandmüller C, Suezer Y, et al. A synthetic human cytomegalovirus pp65-IE1 fusion antigen efficiently induces and expands virus specific T cells. Vaccine. 2017;35(38):5131–5139. doi: 10.1016/j.vaccine.2017.08.019
[14] Berencsi K, Gyulai Z, Gönczöl E, et al. A canarypox vector–expressing cytomegalovirus (CMV) phosphoprotein 65 induces long-lasting cytotoxic T cell responses in human CMV-Seronegative subjects. J Infect Dis. 2001;183(8):1171–1179. doi: 10.1086/319680
[15] Tandon R, Mocarski ES. Control of cytoplasmic maturation events by cytomegalovirus tegument protein pp150. J Virol. 2008;82(19):9433–9444. doi: 10.1128/JVI.00533-08
[16] Paulus C, Nevels M. The human cytomegalovirus major immediate-early proteins as antagonists of intrinsic and innate antiviral host responses. Viruses. 2009;1(3):760–779. doi: 10.3390/v1030760
[17] Sylwester AW, Mitchell BL, Edgar JB, et al. Broadly targeted human cytomegalovirus-specific CD4+ and CD8+ T cells dominate the memory compartments of exposed subjects. J Exp Med. 2005;202(5):673–685. doi: 10.1084/jem.20050882
[18] Cunningham AL, Lal H, Kovac M, et al. Efficacy of the herpes zoster subunit vaccine in adults 70 years of age or older. N Engl J Med. 2016;375(11):1019–1032. doi: 10.1056/NEJMoa1603800
[19] Dagnew AF, Ilhan O, Lee W-S, et al. Immunogenicity and safety of the adjuvanted recombinant zoster vaccine in adults with haematological malignancies: a phase 3, randomised, clinical trial and post-hoc efficacy analysis. Lancet Infect Dis. 2019;19(9):988–1000. doi: 10.1016/S1473-3099(19)30163-X
[20] Anderson TC, Masters NB, Guo A, et al. Use of recombinant zoster vaccine in immunocompromised adults aged ≥19 years: recommendations of the advisory committee on immunization practices — United States, 2022. MMWR Morb Mortal Wkly Rep. 2022;71(3):80–84. doi: 10.15585/mmwr.mm7103a2
[21] Stern L, Withers B, Avdic S, et al. Human cytomegalovirus latency and reactivation in allogeneic hematopoietic stem cell transplant recipients. Front Microbiol. 2019;10:1186. doi: 10.3389/fmicb.2019.01186
[22] Collins-McMillen D, Buehler J, Peppenelli M, et al. Molecular determinants and the regulation of human cytomegalovirus latency and reactivation. Viruses. 2018;10(8):444. doi: 10.3390/v10080444
[23] Krishna BA, Wills MR, Sinclair JH. Advances in the treatment of cytomegalovirus. Br Med Bull. 2019;131(1):5–17. doi: 10.1093/bmb/ldz031

[24] Grifoni A, Sidney J, Zhang Y, et al. A sequence homology and bioinformatic approach can predict candidate targets for immune responses to SARS-CoV-2. Cell Host Microbe. 2020;27(4):671–680.e2. doi: 10.1016/j.chom.2020.03.002

[25] Ong E, Wong MU, Huffman A, et al. COVID-19 coronavirus vaccine design using reverse vaccinology and machine learning. Front Immunol. 2020;11:1581. doi: 10.3389/fimmu.2020.01581

[26] Longhi MS, Hussain MJ, Bogdanos DP, et al. Cytochrome P450IID6-specific CD8 T cell immune responses mirror disease activity in autoimmune hepatitis type 2†. Hepatology. 2007;46(2):472–484. doi: 10.1002/hep.21658

[27] Vita R, Overton JA, Greenbaum JA, et al. The immune epitope database (IEDB) 3.0. Nucleic Acids Res. 2015;43(D1):D405–D412. doi: 10.1093/nar/gku938

[28] Rammensee H, Bachmann J, Emmerich NPN, et al. SYFPEITHI: database for MHC ligands and peptide motifs. Immunogenetics. 1999;50(3–4):213–219. doi: 10.1007/s002510050595

[29] Zhao P, Ma D-X, Yu S, et al. The development of Chinese specific human cytomegalovirus polyepitope recombinant vaccine. Antiviral Res. 2012;93(2):260–269. doi: 10.1016/j.antiviral.2011.12.005

[30] Neto TAP, Sidney J, Grifoni A, et al. Correlative CD4 and CD8 T-cell immunodominance in humans and mice: implications for preclinical testing. Cell Mol Immunol. 2023;20(11):1328–1338. doi: 10.1038/s41423-023-01083-0

[31] Jiang S, Nan F, Zhang S, et al. CRM197-conjugated multi antigen dominant epitope for effective human cytomegalovirus vaccine development. Int J Biol Macromol. 2023;224:79–93. doi: 10.1016/j.ijbiomac.2022.10.105

[32] Araf Y, Moin AT, Timofeev VI, et al. Immunoinformatic design of a multivalent peptide vaccine against Mucormycosis: targeting FTR1 protein of major causative fungi. Front Immunol. 2022;13:863234. doi: 10.3389/fimmu.2022.863234

[33] Zhang Q, Wang P, Kim Y, et al. Immune epitope database analysis resource (IEDB-AR). Nucleic Acids Res. 2008;36(Web Server):W513–W518. doi: 10.1093/nar/gkn254

[34] Backert L, Kohlbacher O. Immunoinformatics and epitope prediction in the age of genomic medicine. Genome Med. 2015;7(1):119. doi: 10.1186/s13073-015-0245-0

[35] Liang YY, Li K-W, Niu F-J, et al. Salvia plebeia R. Br. polysaccharides (SPP) against RSV (respiratory syncytial virus) infection: antiviral effect and mechanisms of action. Biomed Pharmacother. 2021;141:111843. doi: 10.1016/j.biopha.2021.111843

[36] Alzua GP, Pihl AF, Offersgaard A, et al. Inactivated genotype 1a, 2a and 3a HCV vaccine candidates induced broadly neutralising antibodies in mice. Gut. 2023;72(3):560–572. doi: 10.1136/gutjnl-2021-326323

[37] Nelson CS, Jenks JA, Pardi N, et al. Human cytomegalovirus glycoprotein B nucleoside-modified mRNA vaccine elicits antibody responses with greater durability and breadth than MF59-adjuvanted gB protein immunization. J Virol. 2020;94(9):e00186–20. doi: 10.1128/JVI.00186-20

[38] Nan FL, Zheng W, Nan WL, et al. Newcastle disease virus inhibits the proliferation of T cells induced by dendritic cells in vitro and in vivo. Front Immunol. 2020;11:619829. doi: 10.3389/fimmu.2020.619829

[39] Hua J, Stevenson W, Dohlman TH, et al. Graft site microenvironment determines dendritic cell trafficking through the CCR7-CCL19/21 axis. Invest Ophthalmol Visual Sci. 2016;57(3):1457–1467. doi: 10.1167/iovs.15-17551

[40] Hochweller K, Striegler J, Hämmerling GJ, et al. A novel CD11c.DTR transgenic mouse for depletion of dendritic cells reveals their requirement for homeostatic proliferation of natural killer cells. Eur J Immunol. 2008;38(10):2776–2783. doi: 10.1002/eji.200838659

[41] Li C, Lee A, Grigoryan L, et al. Mechanisms of innate and adaptive immunity to the pfizer-BioNTech BNT162b2 vaccine. Nat Immunol. 2022;23(4):543–555. doi: 10.1038/s41590-022-01163-9

[42] Han JC, Li QX, Fang JB, et al. GII.P16-GII.2 recombinant norovirus VLPs polarize macrophages into the M1 phenotype for Th1 immune responses. Front Immunol. 2021;12:781718. doi: 10.3389/fimmu.2021.781718

[43] Ross EA, Devitt A, Johnson JR. Macrophages: the good, the bad, and the gluttony. Front Immunol. 2021;12:708186. doi: 10.3389/fimmu.2021.708186

[44] Sallusto F, Lanzavecchia A, Araki K, et al. From vaccines to memory and back. Immunity. 2010;33(4):451–463. doi: 10.1016/j.immuni.2010.10.008

[45] Ciferri C, Chandramouli S, Donnarumma D, et al. Structural and biochemical studies of HCMV gH/gL/gO and Pentamer reveal mutually exclusive cell entry complexes. Proc Natl Acad Sci USA. 2015;112(6):1767–1772. doi: 10.1073/pnas.1424818112

[46] Chou S, Marousek G, Li S, et al. Contrasting drug resistance phenotypes resulting from cytomegalovirus DNA polymerase mutations at the same exonuclease locus. J Clin Virol. 2008;43(1):107–109. doi: 10.1016/j.jcv.2008.04.005

[47] Hu X, Wang H-Y, Otero CE, et al. Lessons from acquired natural immunity and clinical trials to inform next-generation human cytomegalovirus vaccine development. Annu Rev Virol. 2022;9(1):491–520. doi: 10.1146/annurev-virology-100220-010653

[48] Chen HZ, Tang L-L, Yu X-L, et al. Bioinformatics analysis of epitope-based vaccine design against the novel SARS-CoV-2. Infect Dis Poverty. 2020;9(1):88. doi: 10.1186/s40249-020-00713-3

[49] Weiskopf D, Angelo MA, de Azeredo EL, et al. Comprehensive analysis of dengue virus-specific responses supports an HLA-linked protective role for CD8+ T cells. Proc Natl Acad Sci USA. 2013;110(22):E2046–E2053. doi: 10.1073/pnas.1305227110

[50] Gibson L, Dooley S, Trzmielina S, et al. Cytomegalovirus (CMV) IE1- and pp65-specific CD8+ T cell responses broaden over time after primary CMV infection in infants. J Infect Dis. 2007;195(12):1789–1798. doi: 10.1086/518042

[51] Sacre K, Nguyen S, Deback C, et al. Expansion of human cytomegalovirus (HCMV) immediate-early 1-specific CD8+ T cells and control of HCMV replication after allogeneic stem cell transplantation. J Virol. 2008;82(20):10143–10152. doi: 10.1128/JVI.00688-08

[52] Bunde T, Kirchner A, Hoffmeister B, et al. Protection from cytomegalovirus after transplantation is correlated with immediate early 1–specific CD8 T cells. J Exp Med. 2005;201(7):1031–1036. doi: 10.1084/jem.20042384

[53] Bestard O, Lucia M, Crespo E, et al. Pretransplant immediately early-1-specific T cell responses provide protection for CMV infection after kidney transplantation. Am J Transplant. 2013;13(7):1793–1805. doi: 10.1111/ajt.12256

[54] Kar R, Chattopadhyay S, Sharma A, et al. Single-cell transcriptomic and T cell antigen receptor analysis of human cytomegalovirus (hCMV)-specific memory T cells reveals effectors and pre-effectors of CD8 + - and CD4 + -cytotoxic T cells. Immunology. 2024;172(3):420–439. doi: 10.1111/imm.13783

[55] Sadeghi M, Daniel V, Naujokat C, et al. Dysregulated cytokine responses during cytomegalovirus infection in renal transplant recipients. Transplantation. 2008;86(2):275–285. doi: 10.1097/TP.0b013e31817b063d

[56] Kang S, Brown HM, Hwang S. Direct antiviral mechanisms of Interferon-Gamma. Immune Netw. 2018;18(5):e33. doi: 10.4110/in.2018.18.e33

[57] Ravesloot-Chávez MM, Van Dis E, Stanley SA. The innate immune response to mycobacterium tuberculosis infection. Annu Rev Immunol. 2021;39(1):611–637. doi: 10.1146/annurev-immunol-093019-010426

[58] Inoue T, Kurosaki T. Memory B cells. Nat Rev Immunol. 2023;24(1):5–17. doi: 10.1038/s41577-023-00897-3

[59] Gerlach C, Moseman EA, Loughhead SM, et al. The chemokine receptor CX3CR1 defines three antigen-experienced CD8 T cell subsets with distinct roles in immune surveillance and homeostasis. Immunity. 2016;45(6):1270–1284. doi: 10.1016/j.immuni.2016.10.018

[60] Gebhardt T, Wakim LM, Eidsmo L, et al. Memory T cells in nonlymphoid tissue that provide enhanced local immunity during infection with herpes simplex virus. Nat Immunol. 2009;10(5):524–530. doi: 10.1038/ni.1718

[61] Roark HK, Jenks JA, Permar SR, et al. Animal models of congenital cytomegalovirus transmission: implications for vaccine development. J Infect Dis. 2020;221(Suppl 1):S60–S73. doi: 10.1093/infdis/jiz484